Article

Marine Demonstration of Alternative Fuels on the Basis of Propulsion Load Sharing for Sustainable Ship Design

Hyungwon Shim [1], Yun Ho Kim [1], Jang-Pyo Hong [1], Donghee Hwang [2] and Hee Jin Kang [1],*

[1] Alternative Fuels and Power System Research Center, KRISO, Daejeon 34103, Republic of Korea
[2] Technology and Research Institute, KTE Co., Ltd., Busan 618270, Republic of Korea
*   Correspondence: hjkang@kriso.re.kr; Tel.: +82-42-866-3417

Abstract: As the IMO aims to reduce greenhouse gas emissions from ships by more than 50% by 2050 compared to 2008, the paradigm of the shipbuilding and shipping industries is changing. The use of carbon-free fuels, such as hydrogen and ammonia, is progressing, along with the incorporation of batteries and fuel cells in ships. With the introduction of various propulsion power sources, the application of electric propulsion systems to ships is also expected to accelerate. The verification of reliability and safety is of paramount importance in the development of new technologies designed in response to environmental regulations. However, maritime demonstration is time-consuming and expensive. Therefore, an effective means of demonstrating the performance, reliability, and safety of various marine carbon-neutral technologies with a small burden is required. This study introduces a ship design for marine demonstration, integrating eco-friendly alternative fuels and electric propulsion system components. We further demonstrate a preparation process for the realization of marine carbon neutrality and future ship design through international joint research, standardization, and ship development, which can be linked to manpower training.

Keywords: greenhouse gas regulation; alternative fuels; electrification; electric propulsion; DC switch board

1. Introduction

Environmental issues remain a major global concern, and in 2018, the International Maritime Organization (IMO) set a target to reduce greenhouse gas emissions from ships by 50% by 2050 [1,2]. Alternative marine fuels, such as LNG, methanol, biofuel, and e-fuels, are considered [3–5]. Therefore, many shipyards and shipping companies are developing technologies to comply with greenhouse gas (GHG) regulations. Representative examples of reducing greenhouse gas emissions include optimizing ship hull forms, using energy-saving devices (ESDs), air lubrication systems, slow steaming, and route optimization [6,7]. Although liquefied natural gas (LNG) propulsion systems are known to reduce carbon emissions by about 20% compared to marine fuel oil (MFO)-based systems, they face limitations due to increasingly strict greenhouse gas regulations [8]. It is expected that propulsion power sources will eventually be replaced with carbon-neutral fuels, and that electric/hybrid propulsion systems that can accommodate various propulsion power sources will become more common.

So far, various types of demonstration vessels have been developed in response to GHG regulations, as shown in Table 1. However, designing and building a demonstration ship takes a long time and is expensive. According to research conducted by RICARDO (www.ricardo.com) at the request of the IMO, more than USD 10 billion is expected to be spent on developing eco-friendly ship technology in response to the IMO's greenhouse gas regulations. Furthermore, more than 60% of this cost is projected to be spent on test evaluation and demonstration, to verify the reliability and safety of the developed technology [9].

Table 1. Research for demonstration vessels in response to GHG regulations.

Research Topic	Key Findings	References
Development of a demonstrator ship for IMO greenhouse gas emissions regulations	This study describes the development and testing of a demonstration ship designed to meet IMO greenhouse gas emissions regulations. The ship is equipped with a hybrid propulsion system consisting of a diesel engine and a battery system, and the results of the testing show that the ship can reduce its emissions by up to 70% compared to a conventional ship.	A. Haglind, et al., 2016 [10]
Development and testing of a full-scale battery-powered ferry	This paper presents the design and testing of a full-scale battery-powered ferry. The ferry was equipped with a large battery bank, electric propulsion, and regenerative braking system. The study found that the ferry was able to operate for a full day on a single charge, and it was expected to reduce CO_2 emissions by more than 95% compared to conventional diesel ferries.	J.T. Holen, et al., 2021 [11]
Development of a hybrid LNG-electric propulsion system for a cruise ship	This paper describes the design and testing of a hybrid LNG-electric propulsion system for a cruise ship. The system consisted of two electric propulsion motors, two gas turbine generators, and two LNG engines. The study found that the system was able to reduce CO_2 emissions by up to 30% compared to conventional diesel-electric systems.	P. Carbone, et al., 2021 [12]
Development of an ammonia-fueled tanker ship	This paper presents the design and analysis of an ammonia-fueled tanker ship for zero-emission shipping. The ship is designed to use ammonia as fuel, which produces no greenhouse gas emissions when burned. The results of the analysis show that the ship can operate efficiently and with zero emissions.	S. Seo, et al., 2021 [13]
Development of a hydrogen fuel cell-powered ferry	This paper describes the design and testing of a hydrogen fuel cell-powered ferry. The study found that the ferry was able to operate for up to 12 h on a single tank of hydrogen, and it was expected to reduce CO_2 emissions by more than 95% compared to conventional diesel ferries.	R. Skontorp, et al., 2021 [14]

The purpose of this study is to construct a marine demonstration vessel capable of collectively and rapidly demonstrating various GHG regulatory response technologies, with economic feasibility and commercialization potential through track record acquisition. Establishing a testbed ship as a center for collecting empirical data on different alternative fuels and propulsion system components can greatly contribute to the development of green ship and shipping technologies, by reducing the time and cost required for marine validation.

By applying the research presented in Table 2 on batteries, fuel cells, and electric/hybrid propulsion systems for the proposed marine demonstration vessel, objective and comparable data can be obtained, which can accelerate the practical application of green ship and shipping technologies.

Table 2. Research for alternative fuels and electric/hybrid propulsion systems.

Research Topic	Key Findings	References
Improvement and optimization of inland ship power and propulsion system	This paper discusses the improvement and optimization of inland ship power and propulsion systems. They combined diesel engines, electrical propulsion, and energy storage devices to achieve higher efficiency and reduced emissions.	Z. Du, et al., 2023 [15]
Concept design of a hybrid offshore patrol vessel	The paper presents a concept design of a hybrid offshore patrol vessel (OPV) that integrates various power sources, including diesel engines, electric motors, and renewable energy sources.	A. Ljulj, et al., 2023 [16]
Deployment of electric ships for green shipping	The study investigates the technical, economic, and regulatory challenges of electric ship deployment and provides recommendations for ship owners and operators to overcome these challenges.	W. Wang, et al., 2022 [17]
Multi-energy integrated ship energy management system	The paper proposes a multi-energy integrated ship energy management system based on a hierarchical control collaborative optimization strategy.	Y. Ren, et al., 2022 [18]
Impact of SOFC power generation plant on carbon intensity index for cruise ships	The study finds that the integration of SOFCs can significantly reduce the CII of cruise ships, thus improving their environmental performance.	M. Gianni, et al., 2022 [19]

To achieve maritime decarbonization and expedite the practical application of related research results, it would be particularly advantageous to have a ship capable of accommodating MW-class alternative fuels and electric/hybrid propulsion system components simultaneously for sea trials, especially for large ships subject to IMO GHG regulations. To this end, the marine demonstration vessel in this study is named the Korea Green Ship Testbed (K-GTB). The K-GTB will be used for international joint research, technology standardization, and the training of technical personnel for the realization of marine carbon neutrality. The K-GTB is designed to have the ability to simultaneously mount and demonstrate MW-class alternative fuels and electric/hybrid system components [20].

2. Characteristics of the K-GTB

The propulsion system consists of two permanent magnet (PM) motors, inverters, converters, a DC switchboard, and two LNG DF main generators. The MW-class batteries, fuel cells, and non-carbon fuel mixed combustion internal combustion engines were evaluated for ship applicability, performance, reliability, and safety via assessing the main generator and propulsion load. Figure 1 shows the K-GTB alternative fuel demonstration concept. The shape and specifications of the K-GTB were decided in consideration of the portability of various eco-friendly ship technologies, and their operability in the coastal waters of Korea.

Figure 2 shows the general arrangement of the K-GTB. The marine battery, fuel cell, and non-carbon fuel mixed combustion internal combustion engine are mounted in a separate area around the mid-ship.
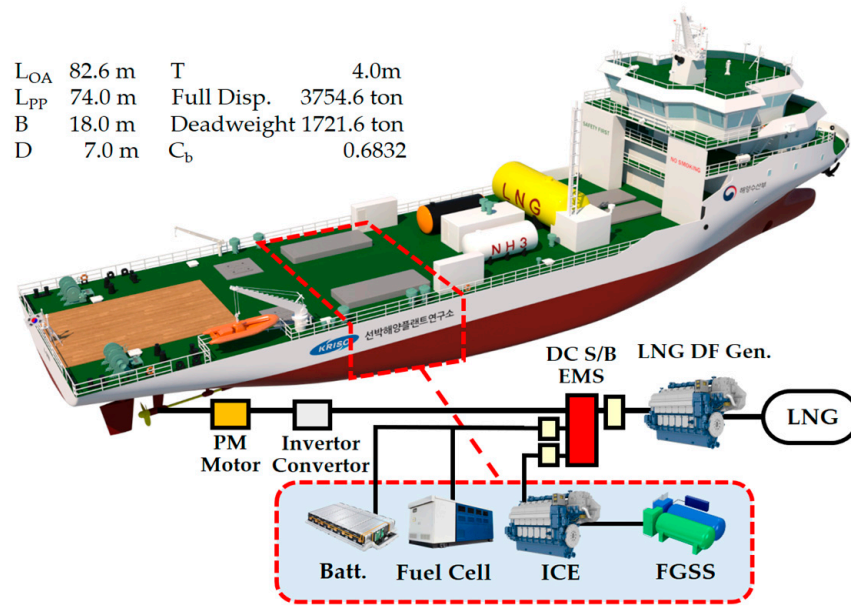
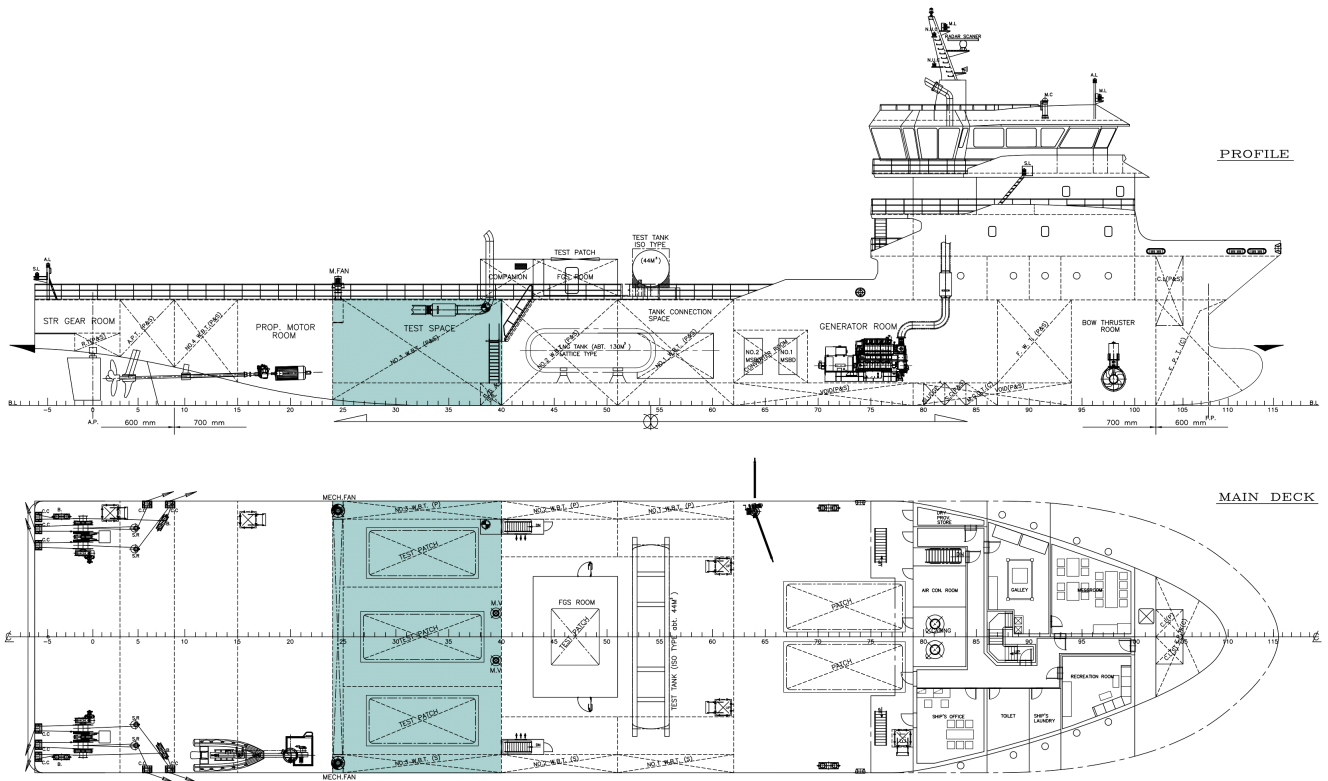**Figure 1.** General arrangement and conceptual diagram of the K-GTB.

Figure 2. General arrangement of the K-GTB (alternative fuels will be installed in shaded areas).

The K-GTB is the first marine demonstration vessel acquired and operated by the KRISO (Korea Research Institute of Ships and Ocean Engineering). It weighs approximately 1722 tons in deadweight, and although it does not reach the scale of full-scale ocean-going cargo ships, its hull form and propulsion structures are similar to those of large cargo ships. In the KRISO, it is possible to acquire all required data from CFD (computational fluid dynamics) analysis, basin model tests, and real-ship operation tests, to be used in various ways to estimate and verify the performance of eco-friendly ship technologies.

3. Ship Resistance Estimation and Propulsion Power Setting

We conducted a review to configure the K-GTB's propulsion system for the demonstration of MW-class batteries, fuel cells, and carbon-free fuel mixed combustion engines. First, the ship resistance characteristics of the K-GTB were evaluated considering both experimental and numerical results. First, calm water resistance was achieved in model tests conducted in KRISO's towing tank, at speeds ranging from 10 kts to 16 kts.

The real ship performance in calm water was then estimated via the ITTC-1978 extrapolation method. The added resistance, induced by waves at different ship speeds, was calculated through a well-known commercial program, WASIM. The essential background of this numerical scheme is explained as follows. As the fluid is inviscid and incompressible, and the flow is irrotational, and the velocity field should satisfy the Laplace equation. The governing equation, the continuity equation, is illustrated in Equation (1). As we adopted the simple Rankine source, only three nonlinear boundary conditions were applied: the body boundary condition (shown in Equation (2)), the kinematic boundary condition (shown in Equation (3)), and the dynamic boundary condition (shown in Equation (4)). Here, we show the velocity potential function, the position vector, the time, the total velocity of a point on the hull, which includes both the steady forward speed and the oscillatory velocity components, the normal vector, the wetted surface of the hull, and the total free surface elevation.

$$\nabla^2 \varphi\left(\vec{x}, t\right) = 0 \tag{1}$$

$$\frac{\partial}{\partial n} \varphi\left(\vec{x}, t\right) = \vec{V}\left(\vec{x}, t\right) \cdot \vec{n} \quad \text{on } S_B \tag{2}$$

$$\frac{\partial}{\partial t} H\left(\vec{x}, t\right) + \nabla \varphi\left(\vec{x}, t\right) \cdot \nabla H\left(\vec{x}, t\right) = \frac{\partial}{\partial z} \varphi\left(\vec{x}, t\right) \quad \text{on z = H} \tag{3}$$

$$\frac{\partial}{\partial t} \varphi\left(\vec{x}, t\right) + \frac{1}{2} \nabla \varphi\left(\vec{x}, t\right) \cdot \nabla \varphi\left(\vec{x}, t\right) = -gH\left(\vec{x}, t\right) \quad \text{on z = H} \tag{4}$$

In the Rankine theory, the velocity potential can be split into four independent potentials: basic, local, memory flow, and incoming wave. Basis flow is assumed to be on the order of one, and is the basis for the linearization. Other flows are assumed to be small perturbations of the basis flow. The formulas, features, and computational algorithms for each flow are illustrated in references [21,22].

The computed meshes of the K-GTB are shown in Figure 3. The section model was converted from the CAD design file, and the sectional hull mesh was generated in three domains: bow, mid-ship, and stern. The additional mesh, the control mesh, was artificially generated under the free surface to calculate the diffracted wave effect.

We initially conducted a test under the conditions of the vessel moving forward in calm water. The ship speed was varied from 0 knots (Knots) to 10 knots, as shown in Table 3. The heave and pitch displacements of the center of gravity were also set to be in the steady-state range. The Froude number was set at a maximum of 0.196, so high Froude number conditions were excluded. As the ship speed increased, the trim of the vessel also increased. Under the highest vessel speed condition, the heave displacement was −0.2 m and the pitch displacement was 1.2 degrees, which resulted in relatively small values. These static changes, according to the ship speed, were used as an initial input value for subsequent calculations.

Next, the resistance induced by waves was calculated. The wave direction was fixed at 180 degrees, and only 2, 6, and 10 knots were used in this study for ship speed. The wavelength was increased from 0.2 to 2.3 compared to the length of the ship. The time series of the added resistance is shown in Figure 4. When the results were stabilized in the latter part of the analysis, the load displacement according to the regular wave was confirmed with five waves.
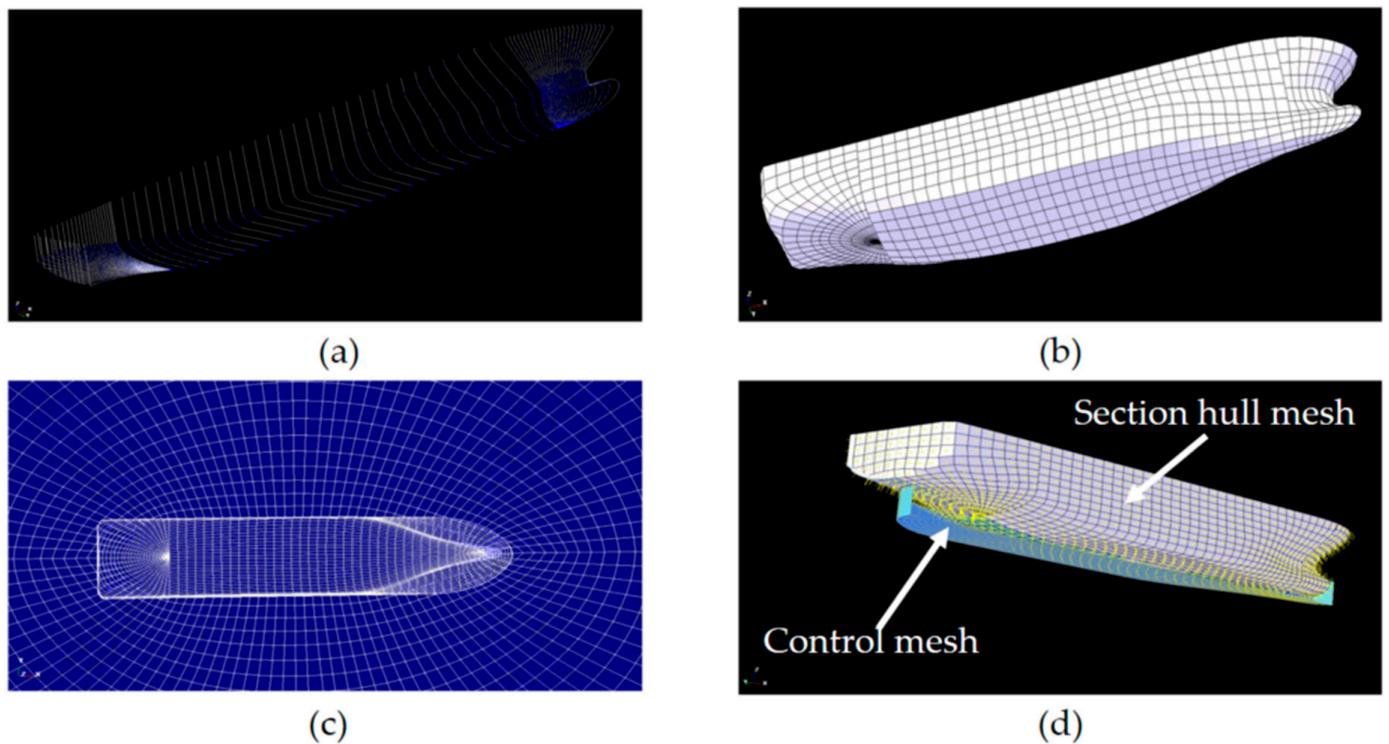
Figure 3. Computational mesh for the three-dimensional panel method (**a**) Sectional Model (**b**) Section Hull mesh (**c**) Control mesh including free surface (**d**) Section hull mesh and control mesh.

Table 3. Calculated equilibrium heel and trim values with forward speeds.

Vs (Knots)	Vs (m/s)	Froude No.	Heave (m)	Pitch (Deg.)
0	0	0	−0.069	0.964
1	0.5144	0.020	−0.070	0.966
2	1.0288	0.039	−0.074	0.971
3	1.5432	0.059	−0.079	0.980
4	2.0576	0.079	−0.087	0.992
5	2.572	0.098	−0.097	1.011
6	3.0864	0.118	−0.110	1.034
7	3.6008	0.137	−0.126	1.062
8	4.1152	0.157	−0.142	1.099
9	4.6296	0.177	−0.164	1.142
10	5.144	0.196	−0.190	1.201

Figure 5 represents the non-dimensional added resistance R_{aw} in the frequency domain, which was normalized by the water density, gravitational acceleration, wave amplitude, the K-GTB's width, and length between perpendiculars ($\rho \times g \times Amp^2 \times B^2/L_{pp}$). The results from the empirical method, STAwave-2 [23], are also shown in this figure for validation. Although relatively similar values were achieved at the slow speed, it was confirmed that the maximum value in the empirical equation was approximately twice as high at the fastest vessel speed. Additionally, the resonance period in the empirical results was generally shorter than that of the 3D Rankine source method. The analysis results suggest that the empirical formula can achieve a higher added resistance than the 3D Rankine panel method. The model test results were evaluated to verify the effect of ship specifications on the ship resistance.
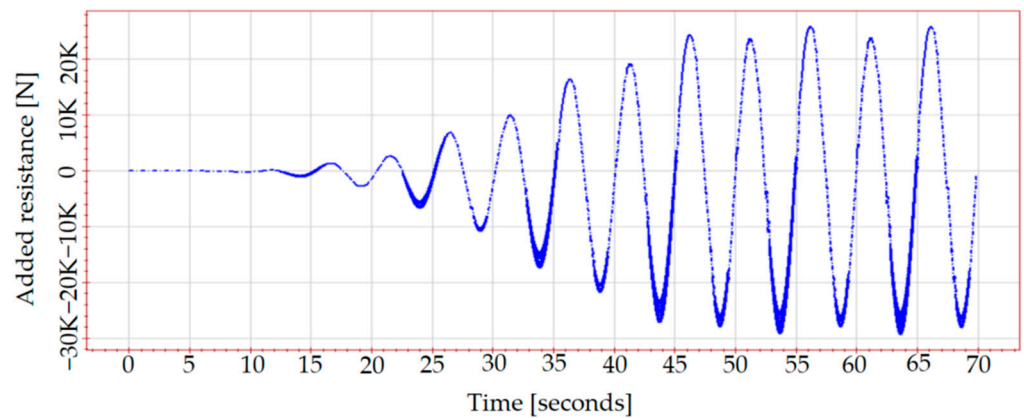
Figure 4. Time series of added resistance at ω = 0.6 rad/s and Vs = 6 kts.

Our results are similar to those of many previous studies, which showed that the empirical formula achieves a relatively high value. In addition, we inferred from the Rankine source method that the amount of trim changes according to the ship speed in the initial stage, and thus the resonance period increases with the length of the ship. Experimental studies should be carried out for a more precise ship load estimation in the future.

In order to consider the total resistance, it is necessary to add the calm water resistance obtained through the experiment. Only extreme conditions of 10 knots or more were tested, due to the limited towing tank slots and the need to evaluate the ship's performance in more dangerous conditions. Therefore, the low speed, reflected in the numerical calculations, was only achieved via extrapolation according to the exponential law. As a result, the calm water resistance was 12.6 kN, 31.1 kN, and 75.0 kN for 2 knots, 6 knots, and 10 knots, respectively.

Added resistance components in the frequency domain were converted into the time domain via Newman's approximation [24]. The considered wave conditions were generated using the JONSWAP spectrum, which is shown in Figure 6. These included a significant wave height of 1.88 m, a peak period of 8.8 s, a wave direction of 180 degrees, and a peak parameter of 2.5, all of which are commonly seen in South Korea.
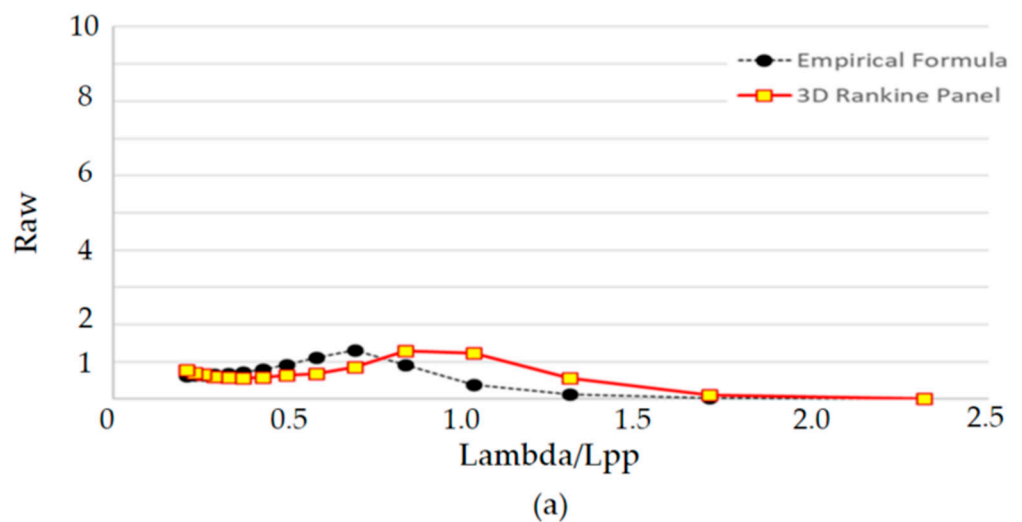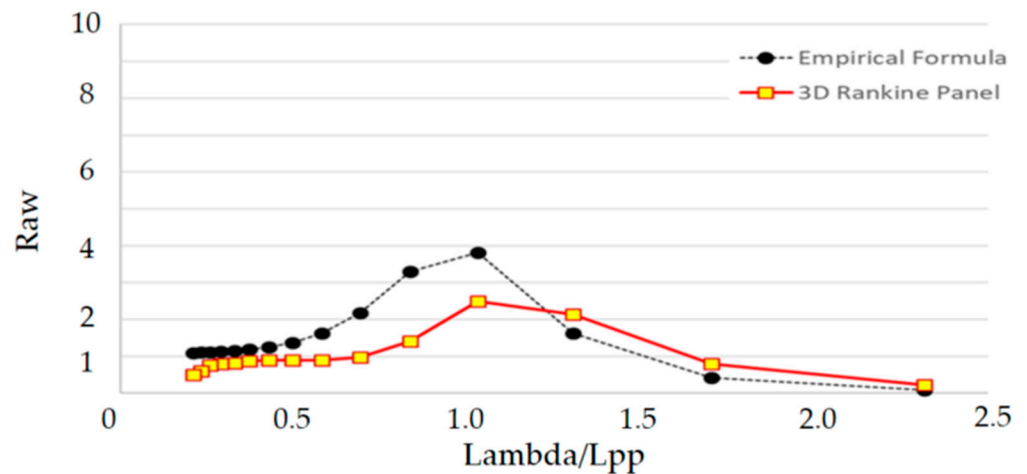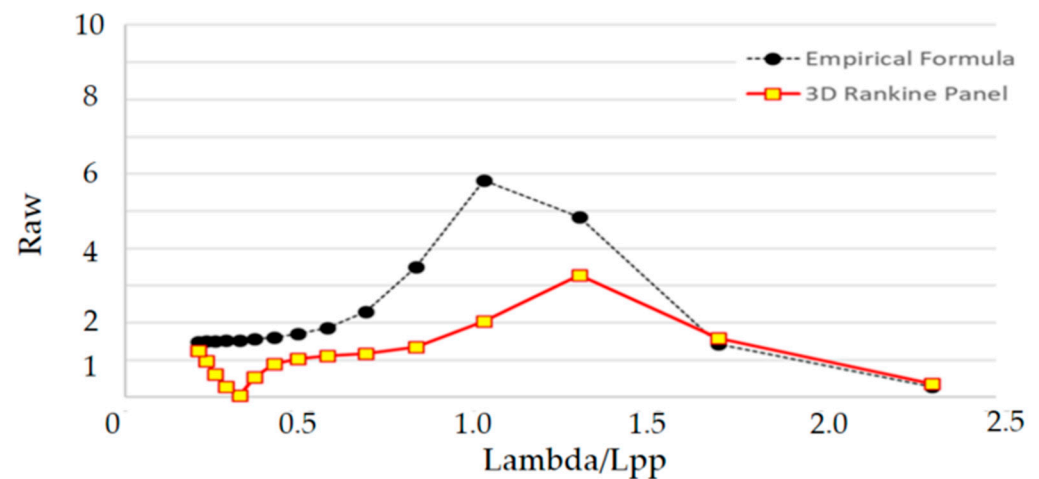

(a)

Figure 5. *Cont.*

Figure 5. Non-dimensional added resistance in a 180 degree heading condition: (**a**) Vs = 2 kts, (**b**) Vs = 6 kts, and (**c**) Vs = 10 kts.

The total resistance of the K-GTB at three different ship speeds is shown in Figure 7, including means and standard deviations. The fluctuation range due to waves was relatively large compared to its resistance in calm water. It was confirmed that the greatest resistance achieved was 270 kN. In the case of the average value, it was confirmed that as the speed increased, a second-order polynomial level was reached. The above results were obtained via the three-dimensional Rankin source method, and are more realistic than the empirical-based estimates. In the future, the time series of these loads will be used as input values for eco-friendly marine fuel system evaluation in the ocean environment.
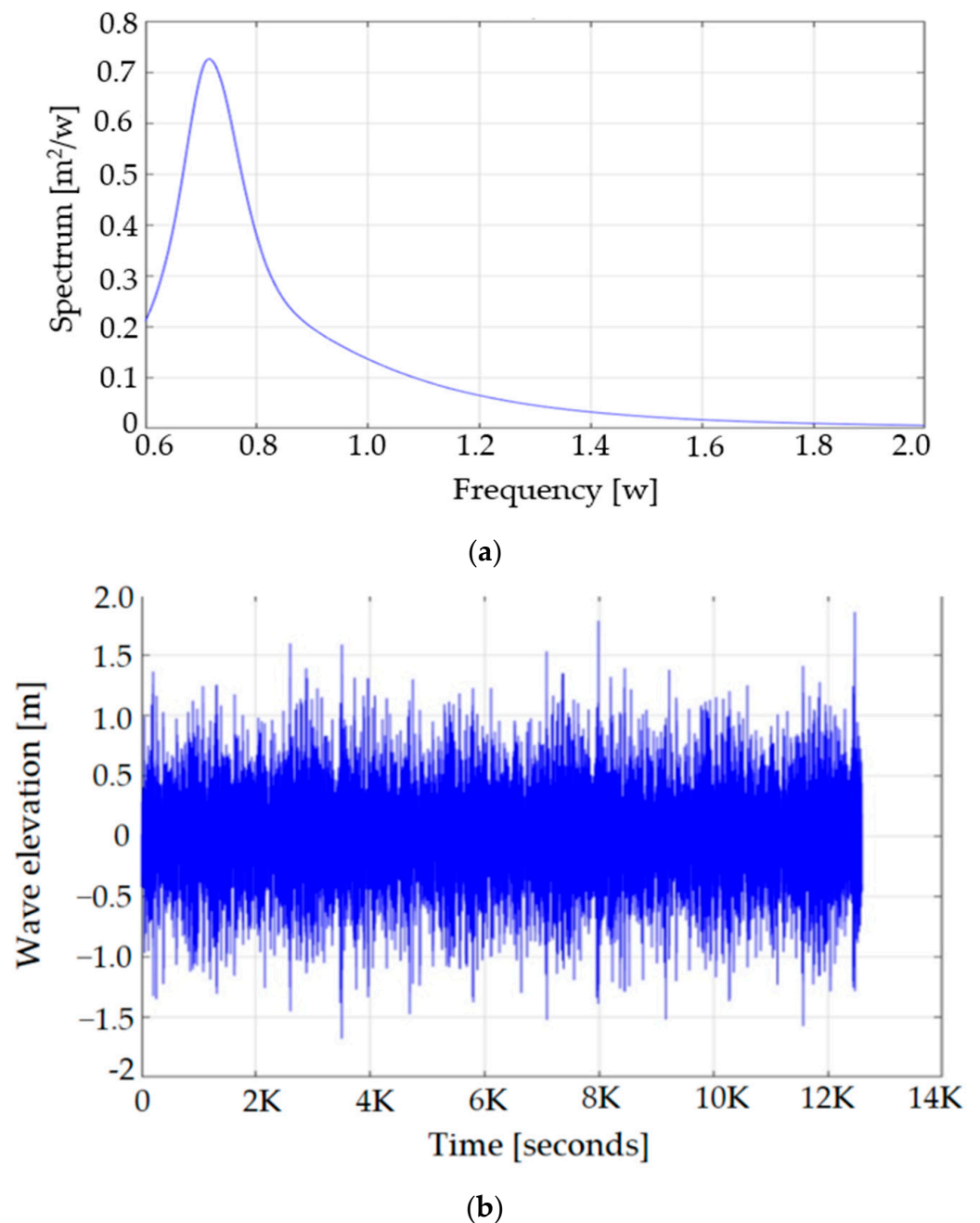
Figure 6. Wave input data: (**a**) JONSWAP wave spectrum and (**b**) wave time series.

Considering the above, the total propulsion power of the K-GTB was set to around 2 MW, to allow it to handle the required propulsion load while operating at a speed of at least 10 knots along the coast of Korea. Afterwards, considering the inner ship space for equipment and the maintainability of the propulsion system, including the PM motor, it was finally decided to install two 1.1 MW PM motors. The K-GTB is expected to be able to achieve a speed of more than 10 knots at 2.2 MW propulsion, even in actual sea operation.

When ammonia or hydrogen fuel is used as fuel for demonstration fuel cells or internal combustion engines, it may be necessary to increase the size of the storage tank due to these fuels' low energy storage density. In preparation for this, we installed a fuel tank for demonstration purposes separately on the open-air deck of the K-GTB, to secure sufficient space for safety reasons [25].
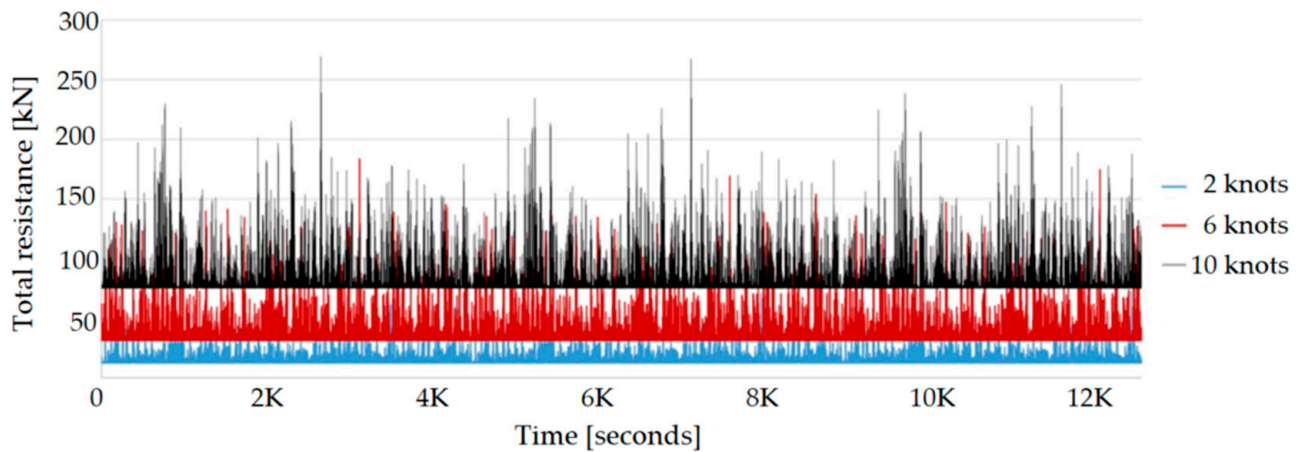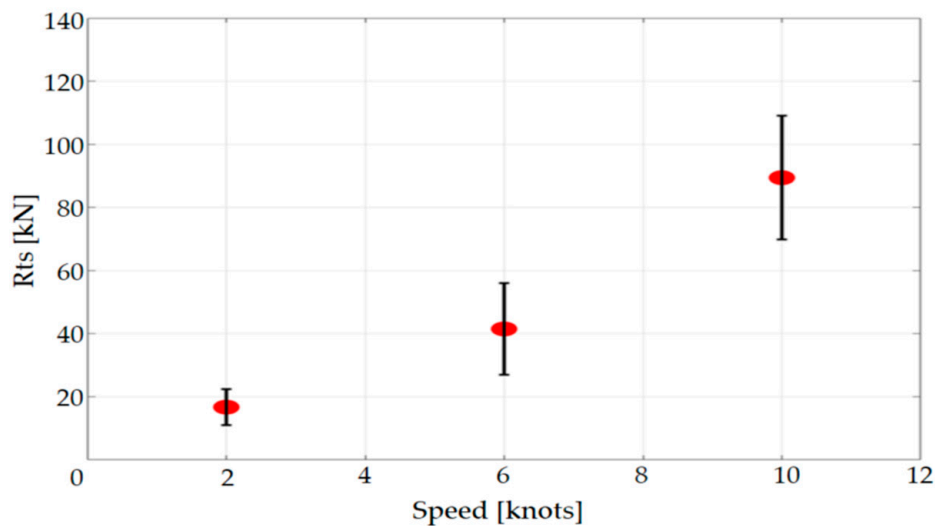
Figure 7. Total resistance (Rts) at different ship speeds; (**a**) total resistance in the time domain, and (**b**) statistical values of total resistance.

4. Marine Demonstration by Load Sharing of Propulsion Power

A hybrid propulsion system that transfers the power generated by two LNG dual-fuel (DF) main generators to two 1.1 MW-class permanent motors (PMs) through a direct current (DC) switchboard was installed in the K-GTB. A DC switchboard was used because it is easy to connect to various propulsion power sources, such as MW-class batteries, fuel cells, and carbon-free fuel hybrid engines, for demonstration. During K-GTB operation, the LNG DF main generator and the alternative fuels to be demonstrated share the propulsion load, enabling the evaluation of various operational profiles.

For example, in the case of MW-class marine battery evaluation, the battery during K-GTB operation is evaluated by increasing the output load shared by one LNG DF generator, from 0 to 100%. The battery system is then assessed for its performance, reliability, and safety under the required charging and discharging conditions, and data related to the shipboard demonstration are secured.

In the future, a separate measurement device for verifying NO_x, SO_2/CO_2 ratio, and CO_2 emissions will be added; however, for this study, the value calculated based on the fuel consumption of the DF main generator, with the use of eco-friendly alternative fuel, was compared with the measured value. The greenhouse gas reduction effect can be calculated or measured by considering the use of alternative fuels and the amount of fossil fuels

used. After securing objectivity through third-party verification, the verification results are reflected in the Energetic Efficiency Design Index (EEDI) and the Energy Efficiency Existing Ship Index (EEXI) formulas.

The K-GTB was designed to enable simultaneous installation of three types of MW-class batteries, fuel cells, and carbon-free fuel mixed engines, as well as the simultaneous demonstration of two or more types of propulsion power sources. The alternative fuel loading area was designed according to the relevant rules of the classification society, and was equipped with an emergency response system (or damage control system), which is an expanded alarm, monitoring, and fire protection system designed to respond to accidents that may occur during the demonstration process [26].

The bus voltage of the main switchboard equipped on the K-GTB was designed to operate at DC 1000 V. This is in consideration of the scalability constraints of the existing DC 750 V system, the construction cost, and the difficulty in obtaining the appropriate components when configuring a system with more than 1000 volts (V). LNG DF generators are reflected as two alternating currents: (AC) 690 V and 1596 kW. These were configured to drive two 1100 kW-class propulsion motors, without the involvement of a separate alternative-fuel-based propulsion power source, for demonstration at a speed of 10 knots or more in actual sea conditions. For port entry and departure support, one bow thruster with a capacity of 550 kW was installed in the bow section. Figure 8 shows the configuration of the K-GTB's propulsion system for the DC-switchboard-based electric load sharing design.
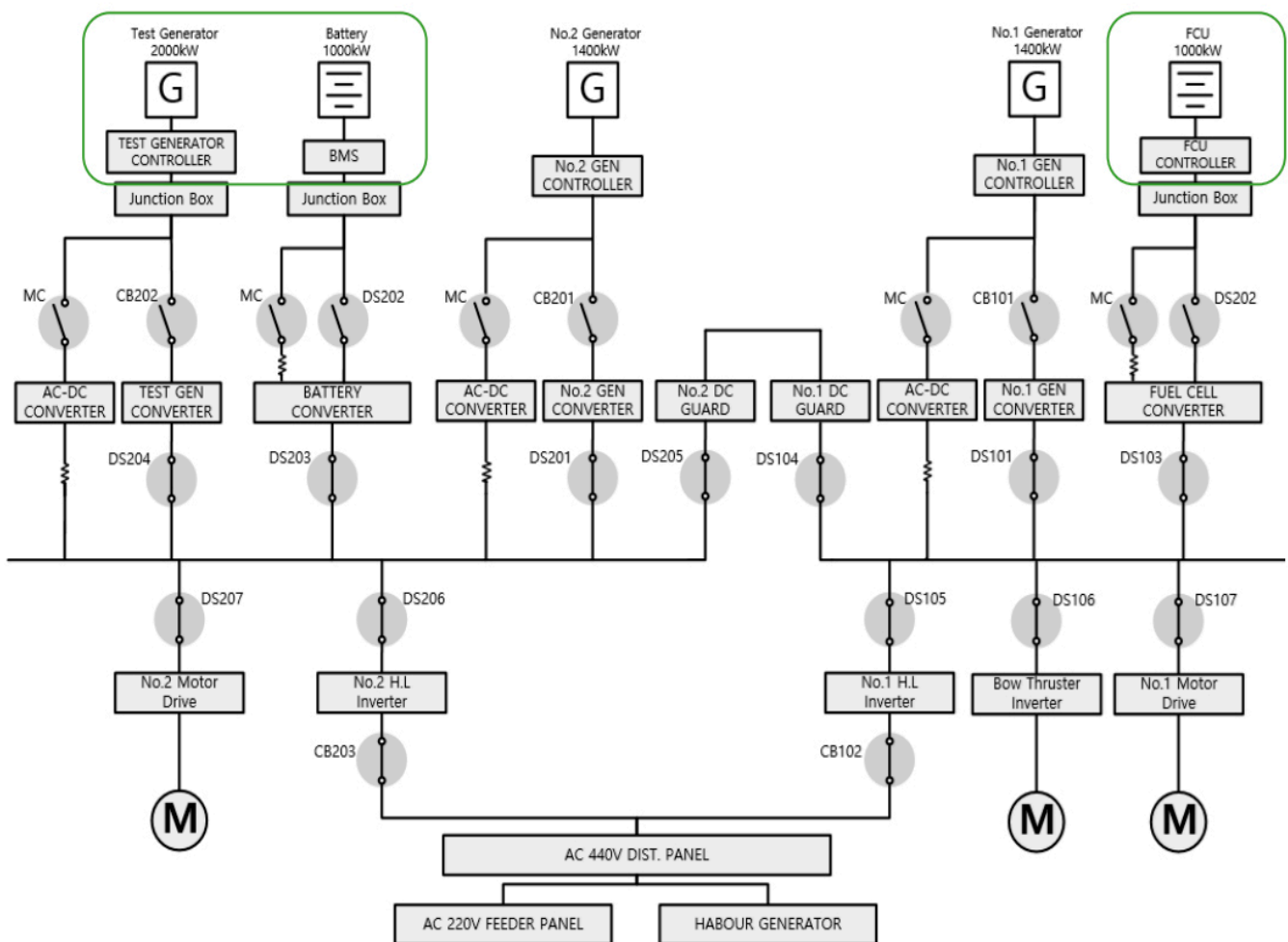

Figure 8. K-GTB propulsion system configuration for DC-switchboard-based electric load sharing (M: electric motor, G: Generator, FCU: Fuel Cell Unit).

In the K-GTB, marine batteries can achieve up to 2000 kW at 770~900 V DC. The fuel cell can achieve up to 1000 kW at 790~900 V DC. The carbon-free hybrid engine can achieve up to 2000 kW at 790~690 V DC. As shown in Table 4, the voltage of the generator on board was finally set at 690 V, after considering the advantages and disadvantages of 450 V and 690 V.

Table 4. K-GTB verifiable battery, fuel cell, and internal combustion engine specifications.

450 V 2000 kW	690 V 2000 kW
■ Required current is approximately 3200 ampere (A) at 450 V PF0.8; ■ Requires four Fl13 modules; ■ Increase in size and cost of main switchboard; ■ A 1692 kW capacity is possible when four Fl13 modules are applied.	■ Required current is approximately 2091 A based on 690 V PF0.8; ■ Requires three Fl13 modules; ■ Cable savings due to reduced current capacity; ■ A 1692 kW capacity is possible when three Fl13 modules are applied.

The K-GTB's propulsion load sharing specifications were set as follows. The connected DC guards, No. 1 bus bar, and No. 2 bus bar were charged, and operated the power grid. Supplying power in the single or parallel mode with No. 1 generator (Gen. 1) and No. 2 generator (Gen. 2) was considered as the base mode. The interval for the best efficiency for Gen. 1 and Gen. 2 was established as 70~90 % of the rated output. Achieving a high efficiency of the alternative fuel power source, the eco-friendly power source (EFPS), depends on the conditions of the test and the test subject. The operating section of the EFPS, subject to verification, depends on the conditions of the test and the test subject. In considering the main bus connection situation of multiple EFPSs, the provision of power to the main bus with only the EFPS was prohibited.

The operation mode is divided into two types: the base mode in which only Gen. 1 and Gen. 2 are operated as propulsion power sources, and the test mode, in which the EFPS is operated as well (preparation, status transition, and EFPS operation modes).

When converting from the base mode to the test mode, a preparation step (test preparation) is performed, to ensure safety and smooth switching between modes. Table 5 shows the operating modes, and Figure 9 shows the process of switching between modes.

Table 5. Propulsion system operation mode of the K-GTB.

Operation Mode	Description	Operable PMS Mode
[M1] base mode	In the case of operating Gen. 1 and/or Gen. 2 with main bus power supply	Single running Parallel running
[M2] status transition mode	A transition step during the EFPS test or after the test that changes the operation mode, checking the status and moving the load	Single running Parallel running
[M3] EFPS mode	Gen. 1/Gen. 2 is responsible for the minimum load required for the bus bar, and EFPS operates according to the load required for the demonstration	Parallel running

Figure 10 shows the diagram of the propulsion system configuration which manages power for the K-GTB. Gen. 1 and Gen. 2 operate alone or in parallel, and both supply power to the K-GTB. Figure 10a shows Gen. 1 as a single operation mode with Gen. 2 in a standby state. Figure 10b shows Gen. 2 as a single operation mode with Gen. 1 in a standby

state. Figure 10c shows Gen. 1 and Gen. 2 in parallel operation. Symmetric mode, asymmetric mode, and fixed mode were considered for PMS modes available in parallel operation.
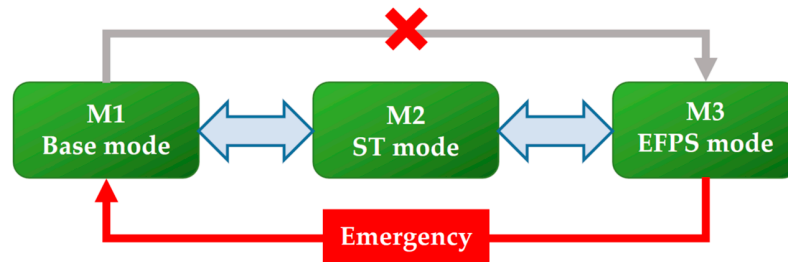

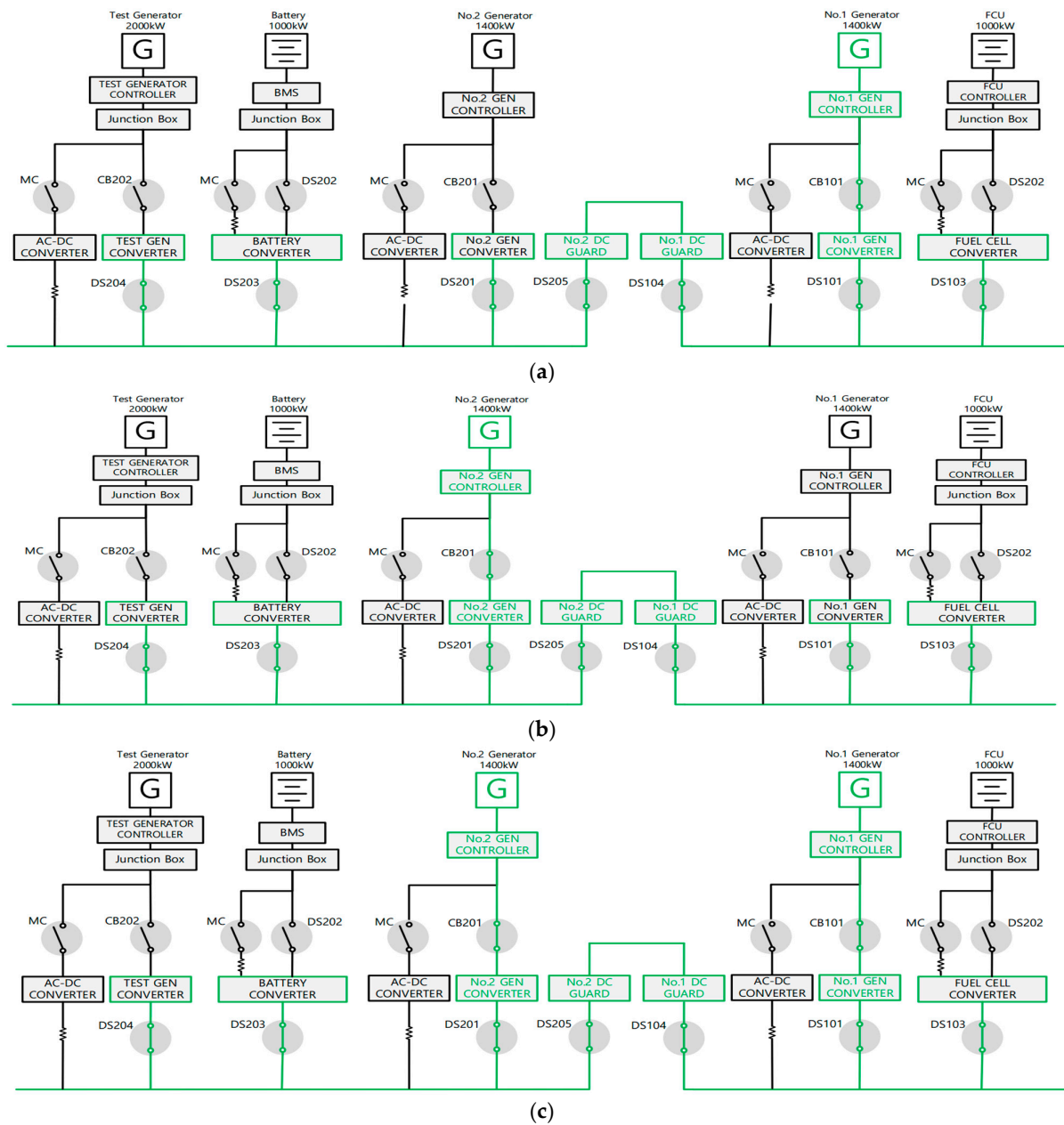**Figure 9.** Conceptual diagram of the power operation mode transition of the K-GTB.

Figure 10. Examples of the K-GTB's propulsion system operation modes; (**a**) Gen. 1 as a single operation mode with Gen (**b**) Gen. 2 as a single operation mode with Gen. 1 in a standby state (**c**) Gen. 1 and Gen. 2 in parallel operation.

The power operation mode is divided into a single mode that uses only the main generator, and a parallel mode that receives power from alternative fuel for demonstration. During operation for marine demonstration, each mode can be transitioned into the other.

Setting the status transition mode to enter the EFPS mode from the base mode can be performed as follows.

- Preprocess
  ※ It is mandatory to input operation-related information for the EFPS and check the connection of the target.
- Step 1: Gen. 1(2) minimum load condition set up
  Gen. 1(2) switch to a single running state and proceed with load reducing:
  {Gen. 1(2) load target level = Gen. 1(2) minimum load + EFPS minimum required load} ... (Equation (1)).
- Step 2: EFPS preparation
  EFPS start-up and preparation: EFPS is ready to connect.
- Step 3: Status check (Always)
  Check for alarms or warnings and take action when necessary:

  (i)   Switch to base mode in the case of alarm/emergency with flag.
  (ii)   Wait for user response when alert occurs with flag.

- Step 4: Waiting for operator confirmation
  Wait for the operator to accept entry into EFPS mode, and continuously check for alarms and warnings. Operator help pop-up.
- END of mode change from base to EFPS mode.
  Next, set the status transition mode to return to base mode from EFPS mode via the following steps.
- Step 1: EFPS load removal
  Cut off the connected load so that the load added to the EFPS for the test reaches the EFPS minimum required load (※ can be achieved according to Gen. 1(2) operation method).
- Step 2: EFPS disconnect
  Block the EFPS and let Gen. 1(2) take the remaining load:
  Gen. 1(2) residual load capacity > EFPS remain load ... (Equation (2)).
- Step 3: Status check (Always)
  Check for alarms or warnings and take action when necessary:

  (i)   Switch to base mode in the case of alarm/emergency with flag.
  (ii)   Wait for user response when alert occurs with flag.

- Step 4: Waiting for operator confirmation
  Wait for the operator to accept entry into EFPS mode and continuously check for alarms and warnings.
- END of mode change from EFPS to base mode.

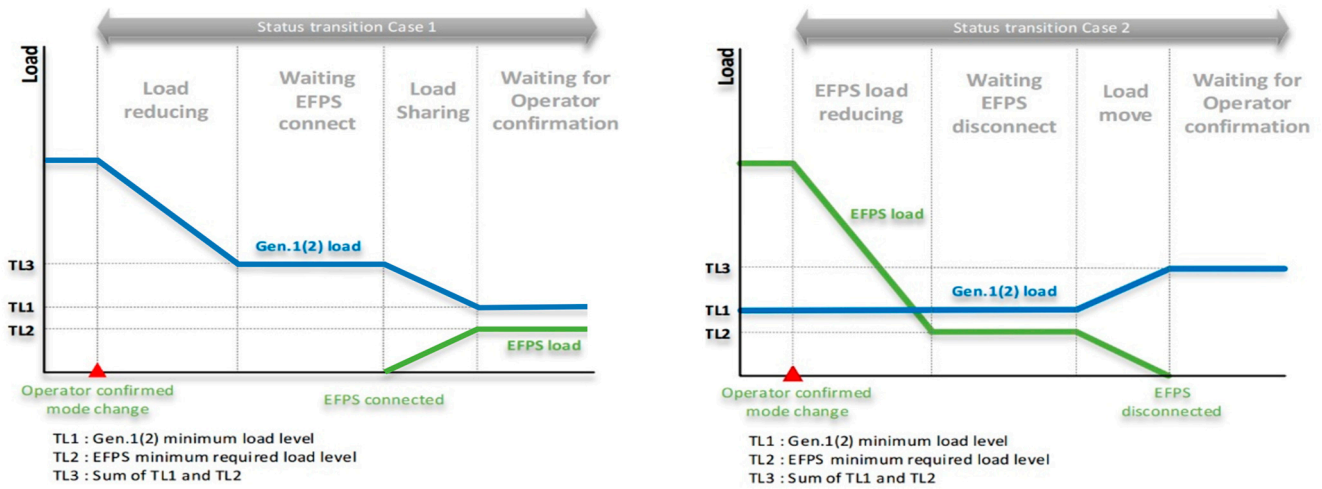 Figure 11 shows the load change process between base mode and EFPS mode.

Figure 11. Diagram illustrating the trends in propulsion load change.

Figure 12 shows the DC switchboard system and the energy management system from the above system design results.
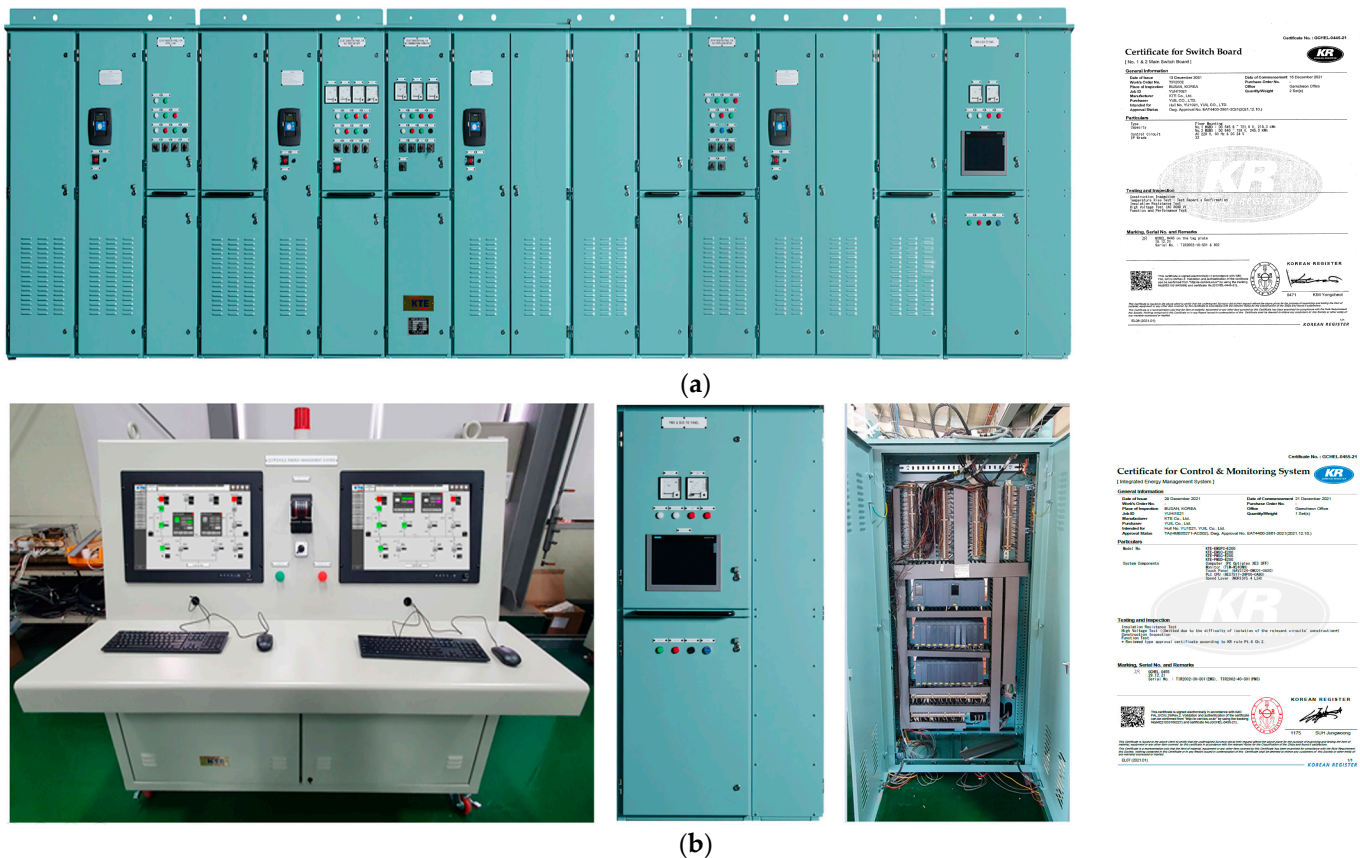

(**a**)

(**b**)

Figure 12. Examples of the developed DC switchboard and energy management system (EMS); (**a**) DC switch board and certification (**b**) Energy Management System (EMS) and certifications.

5. Institutional Considerations

To date, R.O. Korea has no rules for type approval, or related laws for propulsion systems that can change the propulsion power source during operation. Therefore, a temporary exemption from related laws and regulations is required for the marine demonstration of eco-friendly alternative fuel and electric propulsion system components, through the

configuration and utilization of the proposed propulsion system. It is necessary to promote the marine demonstration of developed eco-friendly technologies, secure track records, and promote commercialization. It is possible to secure a verified empirical data technical background for enactment and revision of domestic and international laws.

6. Concluding Remarks

For the development and commercialization of technology designed in response to the IMO's GHG regulations, it is critical to verify the performance, reliability, and safety of new equipment through marine demonstration and to secure track records. On the other hand, the time and cost required for the design, construction, and operation of demonstration vessels is a heavy burden, not only for developing countries, but also for organizations and companies in developed countries. The K-GTB proposed in this study is a marine demonstration vessel that can be used for the development of eco-friendly technologies, with minimum burden of time and cost. The K-GTB is also designed to facilitate international joint research, the dissemination of marine carbon-neutral technology, and information sharing from a model basin test period to real ship operation. In this study, a model test was conducted based on the initial specifications of the K-GTB, and the main propulsion output was set after examining the fluctuation range of the required propulsion power for real sea operation. The main generator and the alternative fuel propulsion power source were designed to share the load required for K-GTB propulsion, using a 1000 V D/C switchboard. The basic design of the K-GTB has been completed, and construction has been in progress since September 2022. The K-GTB is expected to be ready for commercialization in 2025 after a launch in 2024, and is expected to serve as a tool for the realization of marine carbon neutrality. Various technologies designed to meet GHG regulations can be tested, evaluated, and demonstrated with the K-GTB, before application for next-generation eco-friendly ship design.

Author Contributions: Conceptualization, H.J.K.; methodology, Y.H.K., H.S., D.H. and H.J.K.; software, Y.H.K.; validation, J.-P.H. and D.H.; writing—original draft preparation, H.S. and H.J.K.; writing—review and editing, H.J.K. All authors have read and agreed to the published version of the manuscript.

Institutional Review Board Statement: Not applicable.

Informed Consent Statement: Not applicable.

Data Availability Statement: Not applicable.

Conflicts of Interest: The authors declare no conflict of interest.

References

1. IMO(MEPC72). "Resolution MEPC.304(72)." Initial IMO Strategy on Reductin of GHG Emissions from Ships. Available online: https://www.imo.org/en/OurWork/Environment/Pages/Index-of-MEPC-Resolutions-and-Guidelines-related-to-MARPOL-Annex-VI.aspx (accessed on 4 January 2023).
2. IMO(MARPOL). Annex VI, Regulation 22A IMO (MEPC72). "Resolution MEPC.304(72)." Initial IMO Strategy on Reductin of GHG Emissions from Ships. 2018. Available online: https://wwwcdn.imo.org/localresources/en/KnowledgeCentre/IndexofIMOResolutions/MEPCDocuments/MEPC.304(72).pdf (accessed on 4 January 2023).
3. Nikolić, D.; Marstijepović, N.; Cvrk, S.; Gagić, R.; Filipović, I. Evaluation of pollutant emissions from two-stroke marine diesel engine fueled with biodiesel produced from various waste oils and diesel blends. *Brodogradnja* **2016**, *67*, 81–90. [CrossRef]

4. Banawan, A.A.; El Gohary, M.M.; Sadek, I.S. Environmental and economical benefits of changing from marine diesel oil to natural-gas fuel for short-voyage high-power passenger ships. *Proc. Inst. Mech. Eng. Part M J. Eng. Marit. Environ.* **2010**, *224*, 103–113. [CrossRef]

5. Ammar, N.R. An environmental and economic analysis of methanol fuel for a cellular container ship. *Transp. Res. Part D Transp. Environ.* **2019**, *69*, 66–76. [CrossRef]

6. Balcombe, P.; Brierley, J.; Lewis, C.; Skatvedt, L.; Speirs, J.; Hawkes, A.; Staffell, I. How to decarbonise international shipping: Options for fuels, technologies and policies. *Energy Convers. Manag.* **2019**, *182*, 72–88. [CrossRef]

7. Bouman, E.A.; Lindstad, E.; Rialland, A.I.; Strømman, A.H. State-of-the-art Technologies, Measures, and Potential for Reducing GHG Emissions from Shipping—A Review. *Transp. Res. Part D Transp. Environ.* **2017**, *52*, 408–421. [CrossRef]

8. DNV-GL. Maritime Forecast to 2050 (Engergy Transition Outlook 2019). 2019. Available online: https://www.dnv.com/maritime/publications/maritime-forecast-2022/download-the-report.html (accessed on 4 January 2023).

9. IMO(MEPC75). MEPC 75/INF.5 Proposal to Establish an International Maritime Research and Development Board (IMRB). 2019. Available online: https://www.ics-shipping.org/wp-content/uploads/2020/08/proposal-to-establish-an-international-maritime-research-and-development-board-imrb.pdf (accessed on 1 January 2023).

10. Haglind, A.; Sjöström, M.; Brynolf, S.; Wäckelgård, E.; Andersson, M. Development and testing of a demonstrator ship for IMO greenhouse gas emissions regulations. *Proc. Inst. Mech. Eng. Part M J. Eng. Marit. Environ.* **2016**, *230*, 356–366. [CrossRef]

11. Holen, J.T.; Eidsmo Rein, G.; Rekdal, S.L.; Moan, T. Design and testing of a full-scale battery-powered ferry. *J. Mar. Sci. Eng.* **2021**, *9*, 592. [CrossRef]

12. Carbone, P.; De La Fuente, A.; Arnaldo, R.; Fossen, T.I. Design and testing of a hybrid LNG-electric propulsion system for a cruise ship. *Appl. Energy* **2021**, *283*, 116231. [CrossRef]

13. Seo, S.; Son, H.; Kim, Y.; Choi, J.; Kim, D. Design and analysis of an ammonia-fueled tanker ship for zero-emission shipping. *J. Mar. Sci. Eng.* **2021**, *9*, 1296. [CrossRef]

14. Skontorp, R.; Skarphagen, H.; Molnes, A.R. Design and testing of a hydrogen fuel cell-powered ferry. *J. Mar. Sci. Eng.* **2021**, *9*, 697. [CrossRef]

15. Du, Z.; Chen, Q.; Guan, C.; Chen, H. Improvement and Optimization Configuration of Inland Ship Power and Propulsion System. *J. Mar. Sci. Eng.* **2023**, *11*, 135. [CrossRef]

16. Ljulj, A.; Slapničar, V.; Grubišić, I.; Mihanović, L. Concept Design of a Hybrid Offshore Patrol Vessel. *J. Mar. Sci. Eng.* **2023**, *11*, 12. [CrossRef]

17. Wang, W.; Liu, Y.; Zhen, L.; Wang, H. How to Deploy Electric Ships for Green Shipping. *J. Mar. Sci. Eng.* **2022**, *10*, 1611. [CrossRef]

18. Ren, Y.; Zhang, L.; Shi, P.; Zhang, Z. Research on Multi-Energy Integrated Ship Energy Management System Based on Hierarchical Control Collaborative Optimization Strategy. *J. Mar. Sci. Eng.* **2022**, *10*, 1556. [CrossRef]

19. Gianni, M.; Pietra, A.; Coraddu, A.; Taccani, R. Impact of SOFC Power Generation Plant on Carbon Intensity Index (CII) Calculation for Cruise Ships. *J. Mar. Sci. Eng.* **2022**, *10*, 1478. [CrossRef]

20. IMO(MEPC 78). MEPC 78-INF.24-Marine Testbed Ship for Alternative Fuels and Electric Propulsion Systems. 2022. Available online: https://www.imokorea.org/upfiles/board/45.%20MEPC%2078%20%B0%E1%B0%FA%BA%B8%B0%ED%BC%AD%28%BF%B5%BE%EE%29.pdf (accessed on 4 January 2023).

21. Fonseca, N.; Guedes Soares, C. Time domain analysis of large amplitude vertical motions and wave loads. *J. Ship Res.* **1998**, *42*, 100–113. [CrossRef]

22. DNV. Software Suite for Hydrodynamic and Structural Analysis of Renewable, Offshore and Maritime Structures. DNV. 12th Aug. 2022. Available online: https://www.dnv.com/Images/Sesam-Feature-Description_tcm8-58834.pdf (accessed on 4 January 2023).

23. ITTC. ITTC-Recommended Procedure and Guidelines: Analysis of Speed/Power Trial Data. International Towing Tank Conference. 7.5-04-01-01.2, 1-33. 2014. Available online: https://ittc.info/media/4210/75-04-01-012.pdf (accessed on 4 January 2023).

24. Newman, J.N. *Marine Hydrodynamics*; The MIT Press: Cambridge, MA, USA, 2018; p. 448.

25. De Vries, N. Safe and Effective Application of Ammonia as a Marine Fuel. Master's Thesis, Delft University of Technology, Delft, The Netherlands, 2019.

26. Lee, D.; Kim, S.; Lee, K.; Shin, S.C.; Choi, J.; Park, B.J.; Kang, H.J. Performance-based on-board damage control system for ships. *Ocean. Eng.* **2021**, *223*, 108636. [CrossRef]